

Light-flavour hadron production in pp and Pb–Pb collisions in the ALICE experiment at the LHC

Francesco Barile^{1,2,a} for the ALICE Collaboration

¹Università degli Studi Di Bari

²Sezione INFN, Bari, Italy

Abstract. Nuclear matter under extreme conditions of temperature and density can be investigated in ultra-relativistic heavy-ion collisions. The measurement of transverse momentum (p_T) distributions and yields of identified particles is a fundamental step in understanding collective and thermal properties of the matter produced in such collisions. At intermediate transverse momentum, it allows for testing the "recombination models" where hadrons could be formed by the coalescence of quarks from a deconfined quark-gluon plasma (QGP). At higher transverse momenta, particle spectra allow one to investigate the mechanism of parton energy loss in the hot and dense hadronic medium. The measurement of spectra in pp collisions not only provides the baseline for the heavy-ion data but also allows for the tuning and optimization of QCD-inspired models. The latest ALICE results on identified and inclusive light-flavour charged particles in pp collisions at $\sqrt{s} = 0.9, 2.76$ and 7 TeV and Pb-Pb collisions at $\sqrt{s_{NN}} = 2.76$ TeV is reviewed. p_T spectra, yields and ratios in pp as a function of the collision energy is shown and compared to previous experiments and Monte Carlo predictions. Recent Pb–Pb results in different centrality intervals is presented and compared to $\sqrt{s_{NN}} = 200$ GeV Au–Au collisions at RHIC. Comparison with predictions from thermal and hydrodynamic models is also discussed.

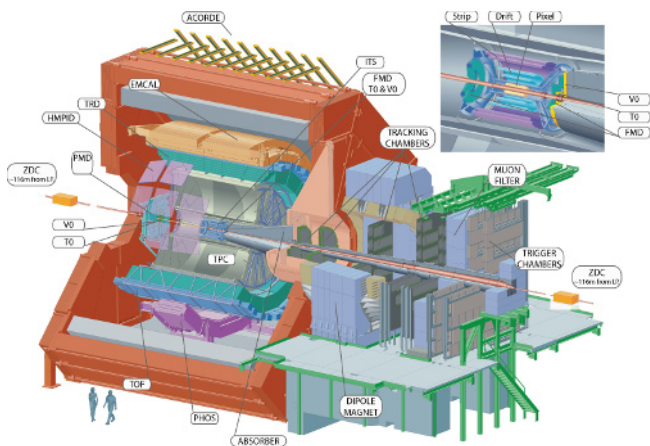


Figure 1. Schematic layout of the ALICE detector with its main subsystems.

1 Introduction

ALICE (A Large Ion Collider Experiment) [1] [2] [3] is a general-purpose heavy-ion detector at the CERN LHC (Large Hadron Collider) devoted to study the physics of strongly-interacting matter and the quark-gluon plasma. It has unique particle identification (PID) capability among the LHC experiments, allowing for the identification of particles in a wide range in p_T . The ALICE experi-

^ae-mail: francesco.barile@cern.ch

ment, shown in figure 1, consists of a central-barrel detector and several forward detector systems. The central system covers the mid-rapidity region $|\eta| < 0.9$ over the full azimuthal angle and it is located inside a solenoidal magnet ($B = 0.5$ T). It includes a six-layer high-resolution inner-tracking system (ITS), a large-volume time-projection chamber (TPC) and electron and charged-hadron identification detectors which exploit transition-radiation (TRD) and time-of flight (TOF) techniques, respectively. A small-area detectors for high- p_T particle-identification (HMPID), photon and neutral-meson measurement (PHOS) and jet reconstruction (EMCal) complement the central barrel. The large-rapidity system includes a single-arm muon spectrometer covering the pseudorapidity range $-4.0 \leq \eta \leq -2.4$ and several smaller detectors (VZERO, TZERO, FMD, ZDC, and PMD) for triggering, multiplicity measurements and centrality determination. Since November 2009 the ALICE detector has collected proton-proton data at several centre-of-mass energy ($\sqrt{s} = 0.9, 2.76, 7$ and 8 TeV) and during the two LHC heavy-ion runs (2010 and 2011) it recorded Pb–Pb collisions at centre-of-mass energy per nucleon pair of $\sqrt{s_{NN}} = 2.76$ TeV. In this paper, recent results on the light-flavour hadron production in pp and in Pb–Pb will be discussed.

2 Particle identification in ALICE

In this section the main particle-identification detector relevant to the analysis presented here are briefly discussed.

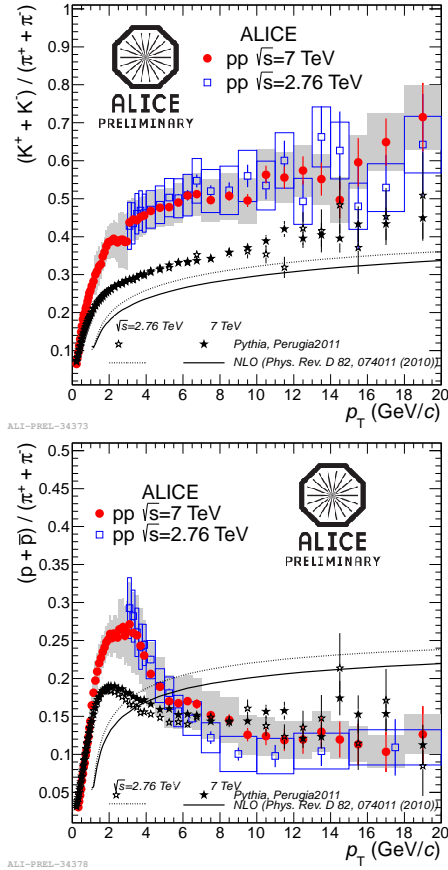


Figure 2. K/π and p/π production ratios in pp collisions at $\sqrt{s} = 2.76$ ($p_T > 3$ GeV/c) and 7 TeV compared to PYTHIA Monte Carlo prediction and NLO calculations.

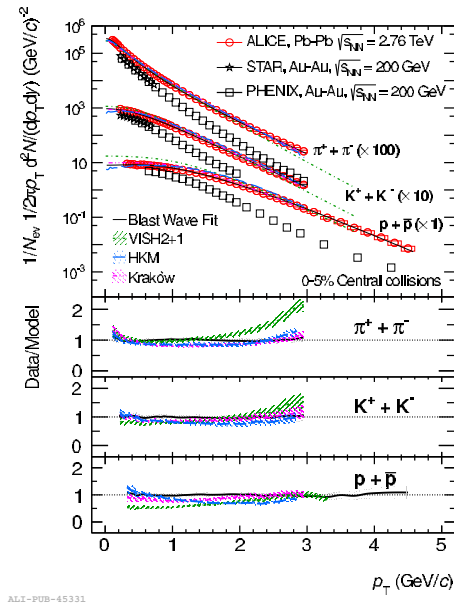


Figure 3. Transverse momentum spectra compared with 3 hydrodynamic models and with the blast wave fit applied separately for each spectrum.

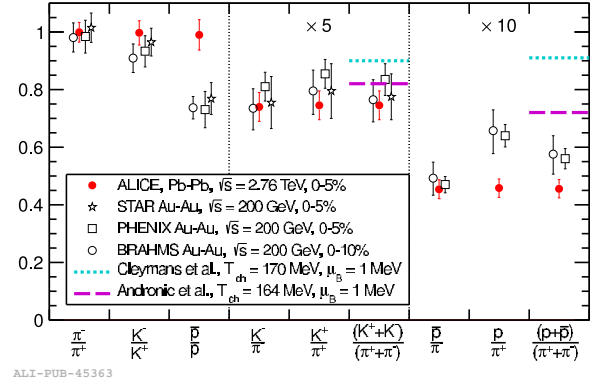


Figure 4. Midrapidity particles ratios, compared to RHIC results and prediction from thermal models for central Pb–Pb collisions at the LHC (combined statistical and systematic errors).

A detailed review of the ALICE experiment and of its PID capabilities are discussed in detail in [1] [2] [3].

The Inner Tracking System (ITS) is a six-layer silicon detector with radii between 3.9 cm and 43 cm providing vertexing and tracking informations. Four of the 6 layers also measure the specific energy loss per unit length (dE/dx) of the particles and are used for particle identification in the non-relativistic region.

The Time Projection Chamber (TPC) [1] [3] is the main central-barrel tracking detector of ALICE. It is a large volume high granularity, cylindrical detector with an outer radius of 2.78 m and a length of 5.1 m. It provides three-dimensional hit information and dE/dx measurement with up to 159 samples. Particle identification is based on the specific energy deposit of each particle in the drift gas of the TPC. It identifies particles in the region of the relativistic rise momenta up to 50 GeV/c.

The Time Of Flight (TOF) [1] [3] detector is a large area array devoted to particle ID in the intermediate momentum range up to 2.5 GeV/c for pions and kaons, up to 4 GeV/c for protons. TOF measures the time of flight of the particles coming from the interaction point with a very good resolution (about 120 ps in pp and 85 ps in Pb–Pb).

The High Momentum Particle Identification Detector (HMPID) [1] [3] [5] enhances the particle identification capabilities of ALICE at higher momenta (pion and kaons up to 3 GeV/c and proton up to 6 GeV/c). It is designed as a single-arm proximity-focusing Ring Imaging Cherenkov (RICH) detector and consists of seven identical counters.

3 Light flavour hadron production

ALICE has measured the yields of produced charged pions, kaons and protons in a wide momentum range and in several colliding systems. The measurements have been performed in pp collisions at several centre-of-mass energies ($\sqrt{s} = 0.9$ [4], 2.76 and 7 TeV) and in Pb–Pb collisions at $\sqrt{s_{NN}} = 2.76$ TeV as a function of collision centrality.

In this section, we present particle ratios and spectra for primary particles, defined as prompt particles produced in

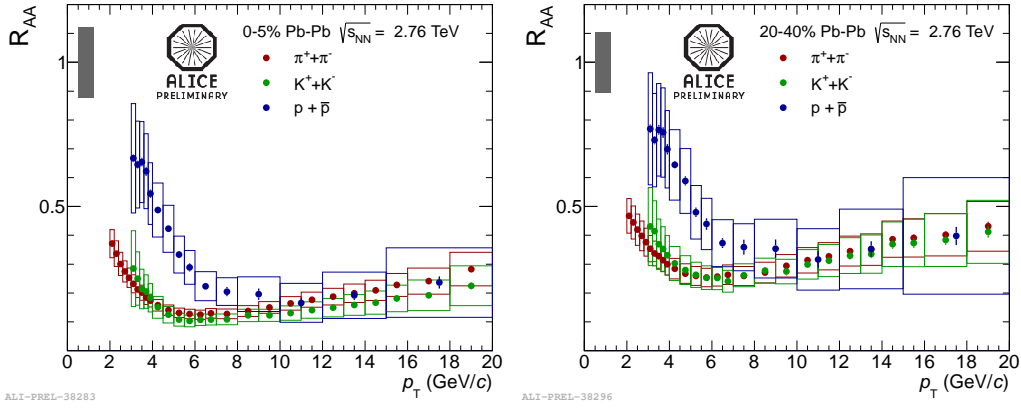


Figure 5. Charged pion, kaon and (anti-)proton nuclear modification factor R_{AA} as a function of p_T for Pb-Pb collisions at $\sqrt{s} = 2.76$ TeV for two centrality bins (0-5% and 20-40%). Statistical and systematic uncertainties are displayed as error bars and boxes, respectively.

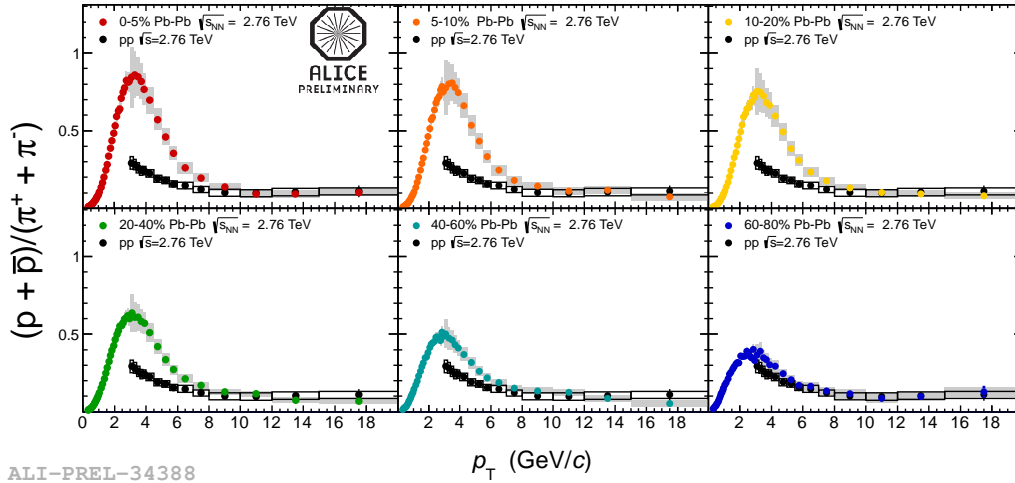


Figure 6. Proton-to-pion ratio in Pb-Pb collisions compared with the pp results at 2.76 TeV in several centrality bins.

the collision and all decay products (except products from weak decays of strange particles). In figure 2, the ratios K/π and p/π as a function of p_T in pp collisions at 2.76 and 7 TeV and different Monte Carlo are shown. They are compared with theoretical model predictions. As it can be seen, both ratios do not show evident energy dependence (within the systematic uncertainties). The ratios are not reproduced by NLO calculations. PHYTIA Monte Carlo generator under estimates the proton-to-pion ratio at intermediate p_T .

In Pb-Pb collisions the p_T distribution of positive and negative particles have been measured and they were found to be compatible within systematic errors. In figure 3 the results are shown for summed charge spectra. The spectra are compared to RHIC results in Au-Au collisions at $\sqrt{s_{NN}} = 200$ GeV [7] [8] and to hydrodynamic models: they show a harder distribution respect to RHIC energies, indicating a significantly stronger radial flow. The spectra have been compared with three different models. A viscous hydrodynamic model VISH2+1 [9], that reproduces well the pion and kaon distributions in $p_T < 1.5$

GeV/c but it misses the protons, both in shape and absolute abundance. The difference is possibly due to the lack of an explicit description of the hadronic phase. This interpretation is supported by the comparison with HKM [10]. Kraków [14] introduces non-equilibrium corrections due to the viscosity at the transition from the hydrodynamic description to particles, which change the effective T_{ch} leading to a good agreement with the data [17] [18]. In order to quantify the kinetic freeze-out parameters, a combined fit with blast-wave [19] function has been performed, with the freeze-out temperature T_{kin} , the average transverse velocity $\langle \beta_T \rangle$ and the exponent of the velocity profile as free parameters. The data are well described by the combined blast wave fit with a collective radial flow velocity $\langle \beta_T \rangle = 0.65 \pm 0.02$ and a kinetic freeze-out of $T_{kin} = 95 \pm 10$ MeV. As compared to fits to central Au-Au collisions at $\sqrt{s_{NN}} = 200$ GeV/c, in similar p_T range, $\langle \beta_T \rangle$ at the LHC is $\sim 10\%$ higher while T_{kin} is comparable within errors [17].

The particle ratios are compared in figure 4 to results at lower energy ($\sqrt{s_{NN}} = 200$ GeV/c) and to the predic-

tion of the thermal model, using $\mu_B = 1$ MeV and a T_{ch} of 164 MeV or 170 MeV. The antiparticle/particle (π^-/π^+ , K^-/K^+ , \bar{p}/p) ratios are all unity within errors, consistent with a vanishing baryochemical potential μ_B . The same ratio (\bar{p}/p) of the yields has been measured by ALICE in pp collisions at $\sqrt{s} = 0.9$ and 7 TeV. The result is consistent with the standard model of baryon-number transport [20]. In figure 4 the K/π and p/π is also shown. The kaon-to-pion ratio is similar to the lower energy values and agrees with the expectations from the thermal model [21]. The proton-to-pion ratio is significantly lower than expected.

In figure 5 [23], the nuclear modification factor R_{AA} for identified charged pions, kaons and (anti-)protons as a function of p_T for two centrality classes (0-20% and 20-40%) is shown. This seems to suggest that, at higher p_T ($p_T > 8 - 10$ GeV/c), the dense medium formed in Pb–Pb collisions does not affect the fragmentation [23].

In figure 6 and figure 7, the proton-to-pion ratio in Pb–Pb collisions in several centrality bins with pp results at 7 TeV is shown. For intermediate p_T it exhibits a relatively strong enhancement, a factor 3 higher than in case of pp collisions at $p_T = 3$ GeV/c. This is reminiscent of the increase in the baryon-to-meson ratio observed at RHIC in the intermediate p_T . The ratio is compatible (within the errors) to the pp value at higher momenta (p_T above 8 - 10 GeV/c) as shown in figure 6.

In figure 7 (top) proton-to-pion ratio in Pb–Pb collisions in several centrality bins compared with pp result at 7 TeV. It is interesting that even in the pp data it exhibits a maximum in the same p_T region as observed in Pb–Pb collisions. In the same figure (figure 7, bottom) proton-to-pion ratio in central Pb–Pb collisions compared with different models. In particular EPOS model [22] shows a good agreement with the data.

4 Summary and conclusions

The most recent results of ALICE experiment on light flavour hadron production both in pp and in Pb–Pb collisions have been reported. The transverse momentum spectra for pions, kaons and protons have been measured with ALICE in several colliding systems and energies at the LHC showing the excellent PID performance capabilities of the experiment and of its sub-systems. In pp collisions, the results show no evident \sqrt{s} dependence in hadron production ratios. In Pb–Pb collisions, the transverse momentum spectra indicate a 10% stronger radial flow than at RHIC experiment. The proton-to-pion ratio is significantly lower than statistical model predictions with a chemical freeze-out temperature $T_{ch} = 160 - 170$ MeV. At intermediate transverse momentum p_T region, an enhancement of the baryon-to-meson ratio is observed. The maximum of the ratio is shifted to higher p_T with respect to RHIC measurement. The nuclear modification factor for pion, kaon and proton has been presented. At higher p_T , this measurement indicates that the medium does not significantly affect the fragmentation.

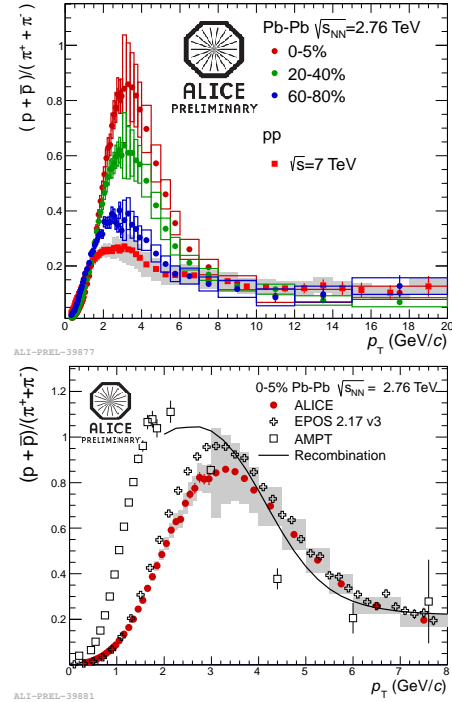


Figure 7. Top: proton-to-pion ratio in Pb–Pb collisions in several centrality bins compared with pp result at 7 TeV. Bottom: proton-to-pion ratio in central Pb–Pb collisions compared with models.

References

- [1] ALICE Collaboration, Physics Performance Report, Volume I, J.Phys.G: Nucl. Part. Phys. 30 (2004) 1517-1763.
- [2] ALICE Collaboration, Physics Performance Report, Volume II, J.Phys.G: Nucl. Part. Phys. 32 (2006) 1295-2040.
- [3] ALICE Collaboration, J.Instrum.3,SO8002 (2008).
- [4] ALICE Collaboration, Production of pions, kaons and protons in pp collisions at $\sqrt{s}=900$ GeV with ALICE at the LHC, Eur.Phys.J.C.71(6); 1655, 2011.
- [5] F. Barile, Inclusive charged hadrons production in pp collisions with the ALICE-HMPID detector at the LHC, <http://cds.cern.ch/record/1517441?ln=it>
- [6] C. Tsallis, J. Stat. Phys. 52, 479 (1988).
- [7] B. Abelev et al. (STAR Collaboration), Phys. Rev. C 79, 034909 (2009).
- [8] S. S. Adler et al. (PHENIX Collaboration), Phys. Rev. C 69, 034909 (2004).
- [9] C. Shen, U.W. Heinz, P. Huovinen, and H. Song, Phys. Rev. C 84, 044903 (2011).
- [10] Y. Karpenko and Y. Sinyukov, J. Phys. G 38, 124059 (2011).
- [11] Y. Karpenko, Y. Sinyukov, and K.Werner, arXiv:1204.5351.
- [12] S. Bass et al., Prog. Part. Nucl. Phys. 41, 255 (1998).
- [13] M. Bleicher et al., J. Phys. G 25, 1859 (1999).
- [14] P. Bozek, Phys. Rev. C 85, 034901 (2012).
- [15] P. Bozek, Acta Phys. Pol. B 43, 689 (2012).

- [16] I. Arsene et al. (BRAHMS Collaboration), Phys. Rev. C 72, 014908 (2005).
- [17] Pion, Kaon and Proton Production in Central Pb–Pb Collisions at $\sqrt{s_{NN}} = 2.76$ TeV. B.Abelev et al. (ALICE Collaboration). 109, 252301 (2012).
- [18] Centrality Dependence of π , K, p Production in Pb–Pb Collisions at $\sqrt{s_{NN}} = 2.76$ TeV. ALICE Collaboration. arXiv:1303.07337v1.
- [19] E. Schnedermann, J. Sollfrank, and U.W. Heinz, Phys. Rev. C 48, 2462 (1993).
- [20] Midrapidity Antiproton-to-Proton Ratio in pp Collisions at $\sqrt{s} = 0.9$ and 7 TeV Measured by the ALICE Experiment. K.Aamodt et al. (ALICE collaboration) DOI: 10.1103 / Phys. Rev. Lett. 105.072002. PRL 105.
- [21] A. Andronic, P. Braun-Munzinger, and J. Stachel, Phys. Lett. B 673, 142 (2009).
- [22] K. Werner, I. Karpenko, M. Bleicher, T. Pierog, and S. Porteboeuf-Houssais, Phys. Rev. C 85, 064907 (2012), arXiv:1203.5704 [nucl-th].
- [23] Nuclear Physics A 904–905 (2013) 763c–766c <http://dx.doi.org/10.1016/j.bbr.2011.03.031>.